Research Square

Preprints are preliminary reports that have not undergone peer review.
They should not be considered conclusive, used to inform clinical practice,
or referenced by the media as validated information.

Frustrated Smectic Liquid Crystal Elastomers as Multifunctional Mechanical Metamaterials

Aidan Street
University of Leeds
Stuart Berrow
s.r.berrow@leeds.ac.uk
University of Leeds https://orcid.org/0000-0003-3764-1613
Zhenming Wang
University of Leeds
Emily Cooper
University of Leeds
Johan Mattsson
University of Leeds https://orcid.org/0000-0001-7057-2192
Helen Gleeson
University of Leeds https://orcid.org/0000-0002-7494-2100

Article

Keywords:

Posted Date: February 6th, 2026

DOI: https://doi.org/10.21203/rs.3.rs-8732550/v1

License: This work is licensed under a Creative Commons Attribution 4.0 International License.
Read Full License

Additional Declarations: Yes there is potential Competing Interest. Stuart R. Berrow, Zhenming Wang, Helen F. Gleeson, have filed a patent related to auxetic smectic LCEs.

Frustrated Smectic Liquid Crystal Elastomers as Multifunctional Mechanical Metamaterials

Author Information

Aidan Street[1§], Stuart R. Berrow[1§*], Zhenming Wang[1], Emily J. Cooper[1], Johan Mattsson[1], Helen F. Gleeson[1]

[1]School of Physics and Astronomy, University of Leeds, Leeds, United Kingdom

[§]These authors contributed equally

*Corresponding author: Stuart R. Berrow (S.R.Berrow@leeds.ac.uk)

ORCiD: A. Street: 0000-0002-7102-7644, S.R. Berrow: 0000-0003-3764-1613, E.J. Cooper: 0009-0007-2440-2492, Z. Wang: 0009-0003-7205-1288, J. Mattsson: 0000-0001-7057-2192, H.F. Gleeson: 0000-0002-7494-2100

Abstract

Auxetics are materials that show a negative Poisson's ratio, i.e. thickening when under strain. The discovery of nematic liquid crystal elastomers (LCEs) as molecular auxetic materials was a paradigm-shift in the design of mechanical metamaterials as they are tuneable, transparent, scalable, non-porous and facile to fabricate. Here, we report that smectic LCEs extend known synthetic molecular auxetics to a second family. The LCEs are acrylate-based, lightly crosslinked (~8 mol%) and polymerised in the nematic phase of a precursor mixture. The resulting smectic-A LCEs exhibit correlation lengths of a few molecular lengths, suggesting layer frustration, which we confirm occurs *via* the mechanism predicted by de Gennes in 1979. Three of the LCEs described exhibit negative Poisson's ratios at strains above ~0.4, thereby marking the first observation of auxetic behaviour in smectic LCEs. Shear oscillatory measurements on the LCEs demonstrate highly anisotropic moduli, which in turn enables elucidation of

highly anisotropic adhesive properties, with differences as large as 20x between geometries. Furthermore, we discern that in the homeotropic case, shear moduli are comparable in both nematic and smectic A LCEs, validating theoretical expectations for such systems.

Introduction

Metamaterials are exciting systems, with properties such as negative refractive indices or coefficients of thermal expansion that are not normally found in nature. Auxetics are a class of mechanical metamaterials that exhibit negative rather than positive Poisson's ratios, meaning they expand under strain rather than contracting, offering mechanical advantages that include resistance to impact, delamination and tear[1,2].So-called re-entrant auxetics, which have been known for several decades, are porous, honeycomb structures in which the auxetic response comes from rotation or deformation of a unit cell wherein volume is not conserved[2]. Large-scale re-entrant auxetic structures have been successfully included in some sportsgear (e.g. running shoes[3] and tennis rackets[4]) but there is no clear route to mass-production of honeycomb structures at sub-micron scales. The discovery of a family of side chain nematic liquid crystal elastomers (Figure 1a and b[5]) as the first synthetic *molecular* auxetics was a breakthrough that transformed the range of possible applications for auxetic materials. In addition to the known benefits of impact and delamination resistance seen by all auxetics, LCEs are the only known transparent[6] auxetics, are scalable from the nanometer regime upwards[7], are highly tunable[8], and offer the potential of facile large-scale manufacture[9]. The auxetic response in nematic LCEs is mediated by a biaxial deformation of the director under strain, accompanied by an out-of-plane molecular rotation which causes a negative Poisson's ratio above a material-dependent threshold strain (usually above ~0.5).[10,11] Intriguingly, it was recently observed that some smectic LCEs also exhibit biaxiality under strain[8,12], but as smectics usually fail at strains above 0.2 - 0.3, which is well below typical auxetic strain-thresholds, an auxetic response was expected to be unachievable. This paper shows that frustrated smectic-A (SmA) systems, which exhibit a

subtle combination of smectic and nematic features, can be strained well beyond 0.3. Auxetic behaviour is observed in the frustrated SmA LCEs, introducing a second materials type to known molecular auxetic systems. The bulk mechanical properties of SmA LCEs differ substantially from nematic variant[13–15] so this discovery represents a broadening of the suite of physical properties in LCEs that might be desirable for applications.

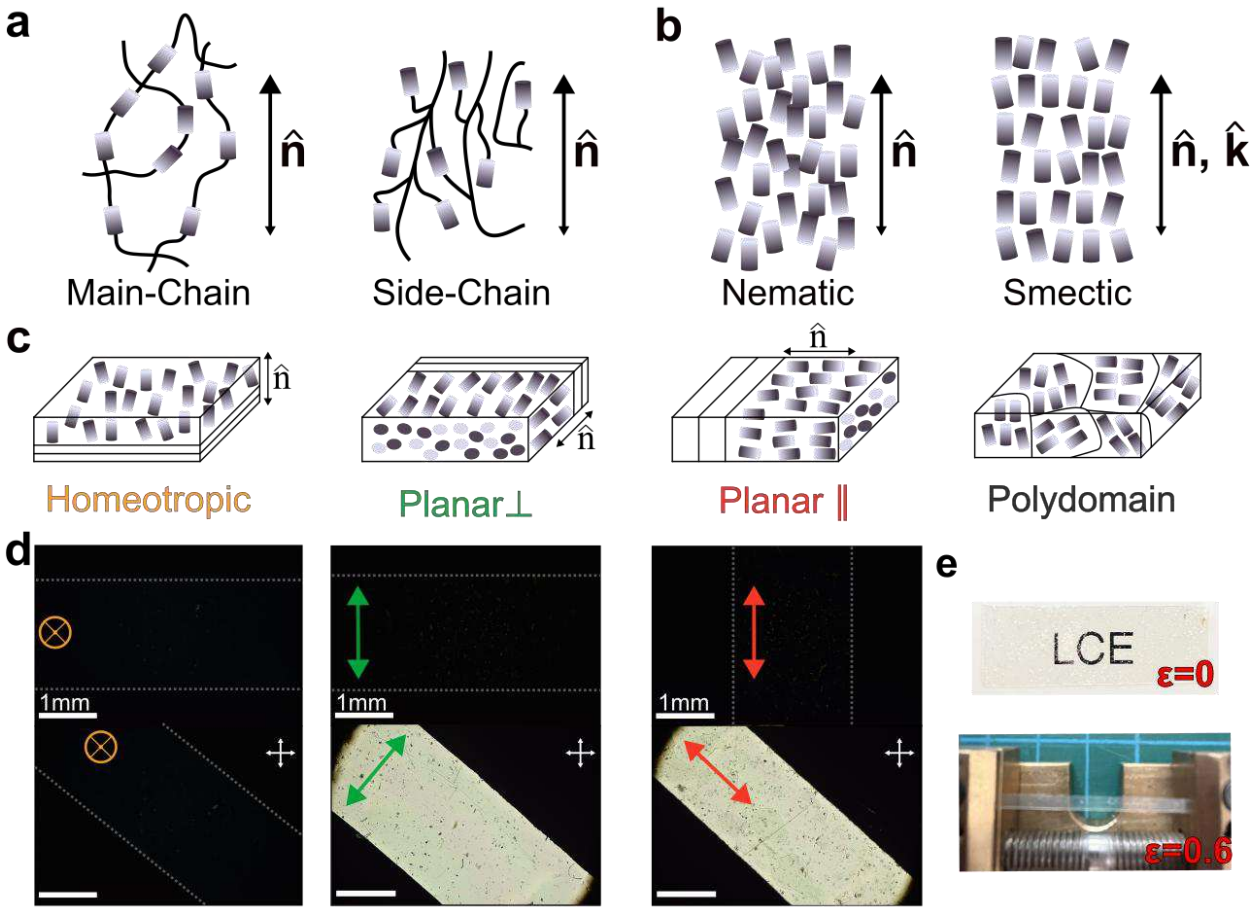


Figure 1 (a) Schematic showing main-chain and side-chain liquid crystal elastomers. (b) The molecular order in the nematic and smectic-A liquid crystal phases, also indicating the director, n̂, and the smectic layer normal, k. (c) Macroscopic geometries typically found in liquid crystal elastomers indicating polydomain, homeotropic and planar geometries. In dynamic mechanical analysis experiments it is appropriate to distinguish between shear perpendicular and parallel to the director in planar geometries, as shown. (d) Polarized microscopy images of LCE3 films in homeotropic and planar geometries demonstrate the high-quality monodomain alignment (a polydomain film would be opaque). The scale bar is 1 mm and the orange, green and red arrows show the director direction. The white arrows indicate the crossed polarizers. (e) (Upper) unstrained LCE3 placed above text reading 'LCE' to show the transparency, (lower) the same LCE in a strain rig at ε = 0.6; the visibility of the rig and backgroundshowcases the transparency under strain.

Liquid crystal elastomers and polymers combine the order of liquid crystals with properties of macromolecular systems, including rubber-like behaviour in the case of elastomers. Such materials have a long history, with the noteworthy discovery of the main chain high-tensile fibre, Kevlar®, in the 1960s followed by significant research activity over the intervening decades that saw the first LCEs synthesized by Finkelmann in the 1980s[15–17]. The field of LCEs strictly stems from de Gennes, who first predicted the extraordinary properties of an elastomer with mesogenic order[18]. A multitude of applications have been suggested to exploit the unique mechanical properties of LCEs, including; impact dampers[19–21]; auxetics[5,6,10]; soft-robotic actuators[22–24]; and smart adhesives[25–28]. However, a further prediction by de Gennes, suggested that templating macromolecules in various liquid crystal phases would modify the resultant mechanical properties[16]. Specifically, he suggested that polymerizing a nematic low molar mass (precursor) system to form a smectic LCE would result in a frustrated smectic layer structure, with mechanical properties that would be distinct from nematic and conventional smectic LCEs. Such an approach is often known as 'templating' and it offers an alternative, largely unexplored, approach to modifying the bulk properties of LCEs[12,29]. We follow this route as an approach to produce SmA LCEs with negative Poisson's ratios.

Berrow *et al.* reported the synthesis of frustrated and conventional SmA structures in acrylate LCEs when studying how changing the condensed phase in which polymerization is conducted effects the properties of the resulting LCEs[12]. The frustrated nature of the SmA phase was identified by a low correlation length which was found to be less than ~5 molecular lengths in those frustrated SmA systems and more than ~10 in the 'true' smectics. It was clear from that work that the two different smectic systems were readily achieved by polymerising in different phases; a nematic precursor tended to form a frustrated SmA LCE, whereas polymerizing in a SmA phase produced LCEs with large correlation lengths, in agreement with de Gennes' prediction[12]. The mechanical properties of these smectic LCEs were explored up to strains of ~0.3; it was shown that the frustrated materials had layer compression moduli that were a factor of ~5 lower than in the conventional SmA LCEs and that they deformed biaxially at low strain. We have now

seen that some of the frustrated SmA LCEs can be strained beyond 0.3 and here we present the large-strain behaviour of those materials, demonstrating that a room temperature auxetic response is realized in some systems where large strains can be achieved. We also present the anisotropic shear moduli of two frustrated SmA materials, one of which is auxetic, allowing us to consider multiple applications of frustrated SmA LCEs. The shear moduli specifically allow one to consider the potential of LCEs as transparent, anisotropic pressure sensitive adhesives, which is another timely application area being considered for nematic LCEs, but which has not yet been reported for smectic systems[25,26,28,30].

Results

Materials

Monodomain films of LCE1, LCE2 and LCE3 were fabricated in both planar and homeotropic geometries (Figure 1 (c) and (d)) and seen to be transparent at strains up to $\varepsilon = 0.6$ (Figure 1 (e)). As the order in LCE4 was induced through an applied mechanical strain, only planar samples were produced. The formulations used are depicted in Figure 2 and the film production methods for all LCEs are described in detail in the methods section. The final films had glass transition temperatures below room temperature in all cases (see Table S1).

Evolution of Smectic Order

In three of the materials considered in this work (LCE1, LCE2, and LCE3), the films were polymerised in a precursor mixture which includes ~50% of a non-reactive liquid crystal 6OCB, included to ensure a room temperature nematic phase. We have previously shown that the final LCE films are SmA, despite the polymerisation being conducted with a nematic precursor mixture[8,12]. These LCEs exhibit a frustrated SmA phase, characterised by relatively short smectic correlation lengths (typically of the order of two to four smectic layers) and they exhibit some nematic-like mechanical properties[12]. The formation of the frustrated SmA phase is explained as a consequence of the distribution of cross-links in the final

elastomer being influenced by the nematic order in the precursor mixture, as suggested by de Gennes[16]. The unreacted 6OCB is washed out after curing and an important question is at what stage the SmA phase forms? Is it during the cure, which would make the LCE consistent with the de Gennes theory, or does it result from the washout step, i.e. the SmA phase is simply the result of a change in composition in the LCE+6OCB phase diagram? The answers to these questions are provided through X-ray scattering studies at each step of the LCE synthesis (Figure 2 b-d).

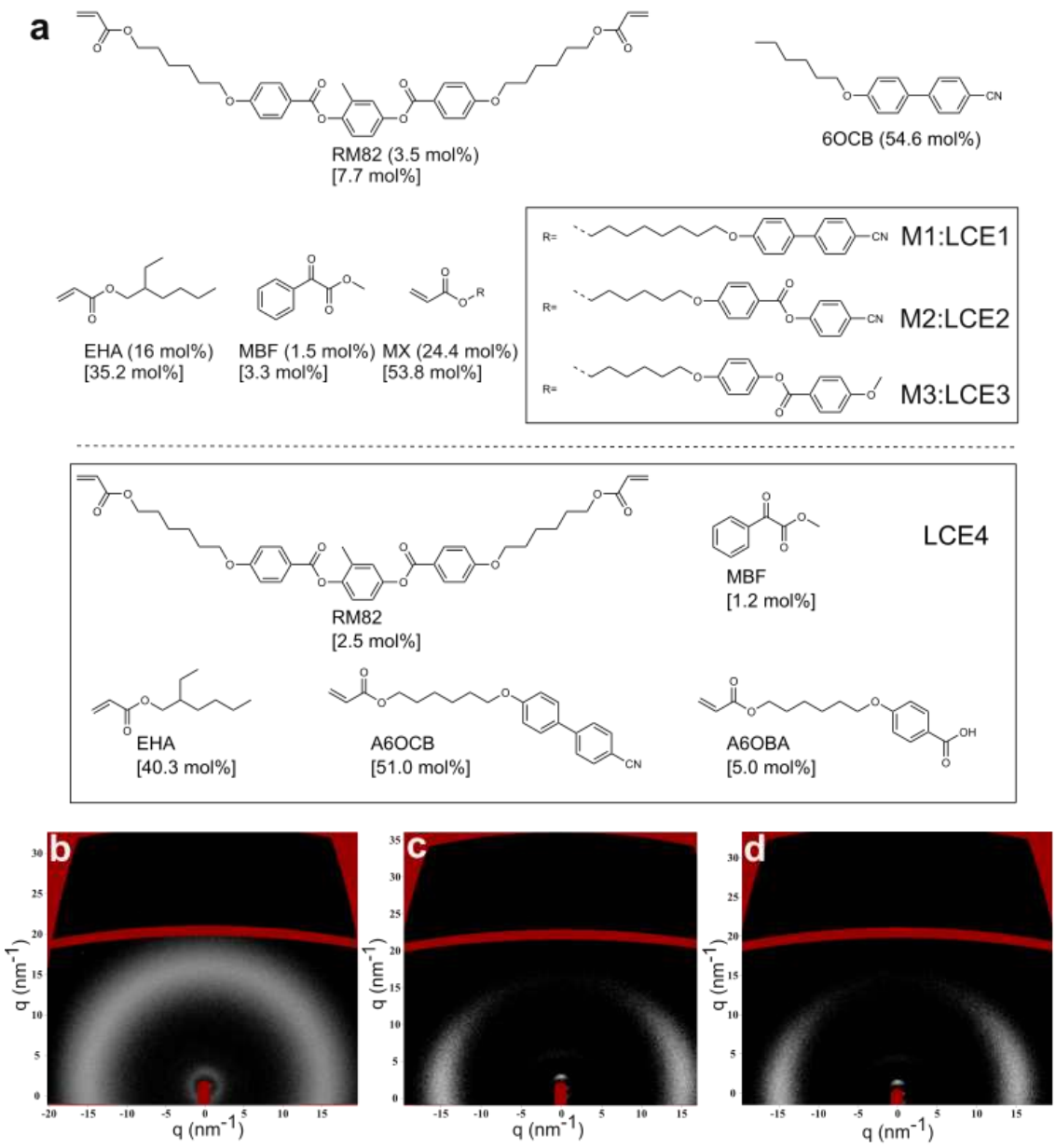


Figure 2. (a) The composition of the LCE mixtures used for the synthesis of the smectic LCEs in this work. The quantities in curved brackets () represent the molar percentage of each component used in the LCE precursor mixtures, and the quantities in square brackets [] represent the molar percentage of the component present in the final LCEs. X-ray scattering data for LCE1 for (b) the precursor mixture, showing a diffuse SAXS peak (c) a planar LCE1 sample after curing but before the removal of 6OCB, and (d) LCE1 after removal of the 6OCB.

We examined the evolution of the smectic ordering in LCE1 through X-ray scattering studies of the unaligned nematic precursor mixture held in a capillary, and aligned samples of the LCE before and after the wash-out step (Figure 2 b-d). The correlation lengths, SmA layer spacing and order parameters

of each LCE, elucidated from x-ray scattering, are given in Table 1. The precursor mixture displays an isotropic-like X-ray scattering pattern as there is no preferred director orientation in the unaligned nematic phase in the capillary. However, the nematic nature of this mixture has been confirmed by differential scanning calorimetry and polarised light optical microscopy (Figures S1 and S3).[8] The formation of the SmA phase upon curing and prior to the removal of 6OCB, Figure 2 (c), is evidenced by a sharp Bragg (001) reflection in the small angle region at $q = 1.83\ nm^{-1}$, together with the orthogonality of the small and wide angle scattering signal (the assignment of the scattering features is indicated in Figure S6). Upon removal of the 6OCB *via* solvent washing, the SmA phase is retained. The orientational order parameter and smectic correlation length in the swollen (unwashed) system (0.62 and 205 Å respectively) are both larger than those observed in the final LCE (0.56 and 161 Å respectively). The higher degree of orientational order in the unwashed sample can be attributed to its higher mesogenic content which is ~80% compared with ~60% in the final LCE. Interestingly, the layer spacing is considerably smaller in the unwashed LCE (34 Å compared with 41 Å), a value that we note is comparable to the 32 Å layer spacing reported for the interdigited structure of 8OCB.[31] This thereby suggests an increased degree of interidigitation of the mesogens in the unwashed sample than is present after the removal of 6OCB.

Mechanical Properties of Frustrated Smectic LCEs

Auxeticity in Smectic LCEs

Nematic molecular auxetic LCEs have been reported to exhibit negative Poisson's ratios above a material- and temperature-dependent threshold strain which is typically ~0.5[5,8,10,32]. The auxetic response has been shown to occur *via* a biaxial deformation that occurs upon straining perpendicular to the liquid crystal director and the circumstances under which a biaxial rather than uniaxial director reorientation occurs have recently been presented[10,11]. Intriguingly, some SmA LCEs have also been seen to deform biaxially though those studies were limited to low strain regimes as similar smectic LCEs had been seen to fail consistently at strains in excess of 0.3[8,12]. Since that work, we have observed that samples of the

some frustrated SmA LCEs are able to withstand strains far in excess of 0.3 prior to failure and, excitingly, they also show an auxetic response.

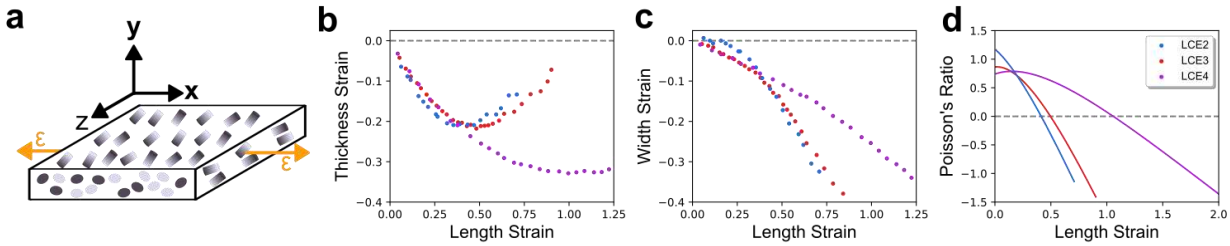


Figure 3. (a) A schematic representation of the experimental conditions employed in the analysis of auxeticity in the LCE samples, defining the naming convention of the x (length), y (thickness) and z (width) axes, where ε represents the applied strain and the rods depict the alignment of the mesogens in the LCE. Panels (b) and (c) show the effect of an applied x-strain on the sample dimension at room temperature in the y-and z-axes respectively. An increase in sample thickness occurs above threshold length strains of 0.41±0.05, 0.50±0.05 and 1.05±0.05 for LCE2, LCE3 and LCE4 respectively. LCE1 consistently failed at strains of ~0.3. d) Shows the instantaneous Poisson's ratio in the y-axis (v) deduced for each sample as a function of the applied x-strain.

Figure 3 shows the effect of a strain applied perpendicular to the director (and layer normal) on the sample dimensions of LCE films of LCE2, LCE3, and LCE4 in the transverse axes. As the strain is applied perpendicular to the initial director, the sample width (*z*-axis in Figure 3(a) and data in Figure 3(b)), decreases throughout the entire strain range, for all the films. However, Figure 3 (c) which shows changes in the sample thickness (*y*-axis in Figure 3(a)), demonstrates completely different behaviour which is reminiscent of the nematic LCEs. The sample thickness initially decreases for all systems but above a threshold value (0.41 ± 0.05, 0.50 ± 0.05, and 1.05 ± 0.05 for LCE2, LCE3, and LCE4, respectively) the sample thickness begins to increase, i.e. the Poisson's ratios (Figure 3 (d)) become negative. These results therefore demonstrate for the first time that when sufficiently high strains can be achieved in some frustrated SmA side-chain LCEs, an auxetic response can be readily observed.

It is noteworthy that the auxetic threshold values of LCE2 and LCE3 are lower than those previously reported for comparable, surface aligned, nematic LCEs (≥0.56)[8,10,32]. Furthermore, it has been previously reported that the auxetic response in nematic LCEs appears to be governed by proximity to the glass transition temperature (T_g) of the sample, with a higher T_g leading to higher auxetic thresholds.[8,33] For the

smectic auxetic LCEs reported here, there is no facile relationship between T_g and the auxetic threshold; LCE2, LCE3 and LCE4 have a T_g of 7 °C, 0 °C and 1 °C respectively (Table S1), with LCE2 having the lowest auxetic threshold (0.41 ± 0.05, compared to 0.50 ± 0.05 and 1.05 ± 0.05 for LCE3 and LCE4 respectively). These results therefore suggest that the auxetic response in smectic LCEs may be influenced by more characteristics than those known to influence the auxetic response in nematic LCEs. Attempts to elucidate these characteristics will be the subject of future studies.

Shear Moduli for Frustrated Smectic LCEs

Despite the similarity of the auxetic response to that in nematic LCEs, it is expected that other aspects of the mechanmechanical behaviour of SmA materials will be quite different. This is because the existence of smectic layers modifies the compression and shear moduli since changes in the smectic layer spacing are generally energetically unfavourable. We chose to examine the mechanical behaviour of two frustrated smectic LCEs through their shear moduli as such measurements offer an approach to also consider their anisotropic adhesion, a behaviour that is of increasing interest as an application area for LCEs[25,26,28]. In particular, here we chose to compare LCE1 and LCE3; although the former could not be strained sufficiently to observe an auxetic response, it allows a direct comparison to adhesion behaviour in an analogous nematic LCE previously reported[28] (with a 6-carbon spacer).

The distinct mechanical behaviour of SmA LCEs is revealed by considering the free-energy density (F) under a shear deformation (Equation (1)), as was originally described in detail by Adams and Warner and is reproduced here for clarity[13].

$$F = \frac{1}{2}\mu Tr\left\{\underline{l}_0 \cdot \underline{\underline{\lambda}}^T \cdot \underline{l}^{-1} \cdot \underline{\underline{\lambda}}\right\} + \frac{1}{2}b\left(\frac{1}{\left|\underline{\underline{\lambda}}^{-T} \cdot n_0\right|} - 1\right)^2 \quad \textbf{(1)}$$

The first term is the same trace formula as in nematic LCEs where μ is the linear shear modulus, $\underline{l}$ the step length tensor which is expressed in terms of the step length anisotropy, r, $\underline{l}$ = Diag(1, 1, r), and $\underline{\underline{\lambda}}$ is the

deformation tensor[13]. The second term relates to the smectic layer spacing, with layer spacing modulus $B = b/\mu$, and the initial director is defined along the z-axis, i.e. $n_0 = (0,0,1)^T$. The expression $1/\left|\underline{\lambda}^{-T} \cdot n_0\right|$ represents the smectic layer spacing d relative to the unstrained spacing d_0, d/d_0.[13,15] Estimates for b and r can be ascertained from thermal expansion and tensile measurements and take values of $r = 2.1 \pm 0.5$ and $b = 7.5 \pm 0.1$, 3.4 ± 0.1, and 5.7 ± 0.1 for LCE1, LCE2, and LCE3 respectively.[8]

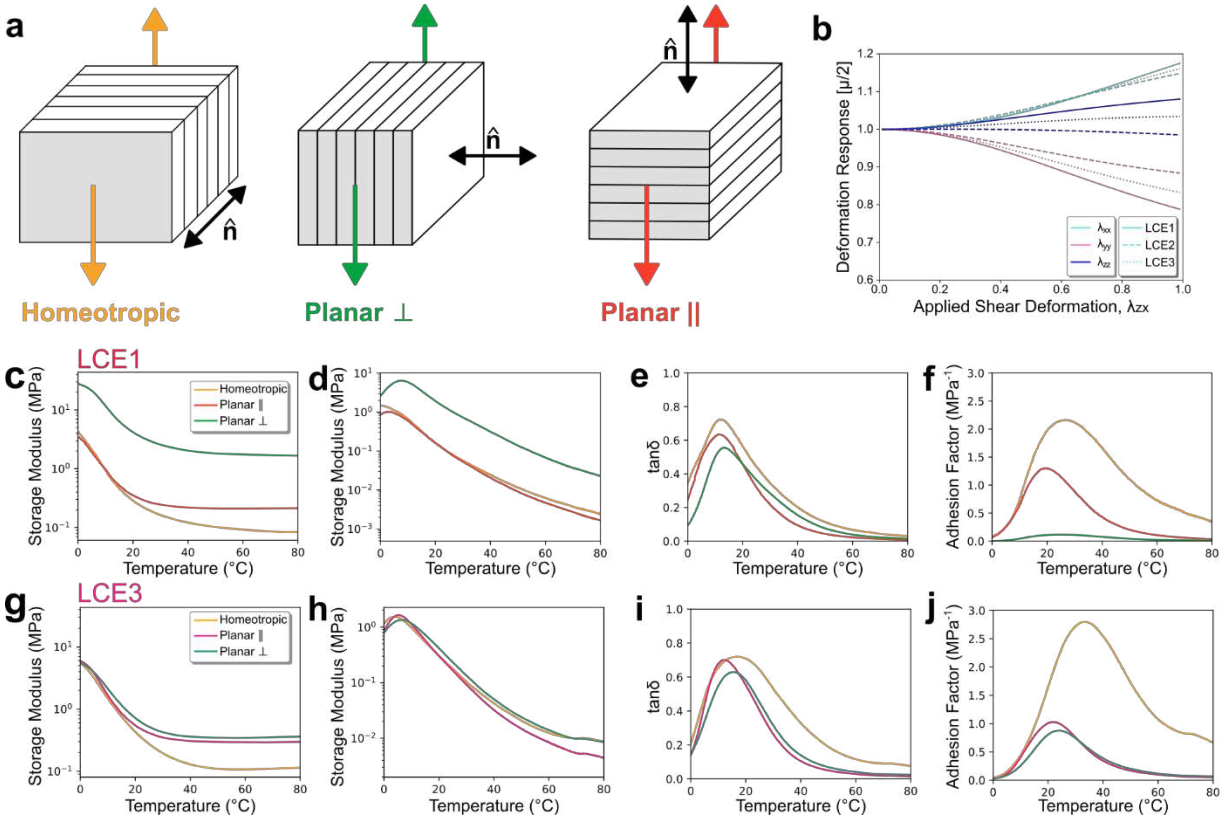


Figure 4. . (a) All possible geometries showing the relationship between the smectic layers and applied shear (arrows), with homeotropic (orange), planar ⊥ (green), and planar ∥ (red). (b) For the planar || case, the applied shear deformation is, λ_{zx} and the minimised principal deformations in λ_{xx} (turquoise), λ_{yy} (pink), and λ_{zz} (blue). The calculation is for a step length anisotropy r = 2.1 and smectic layer compression moduli b = 7.5 (solid), b=3.4 (dotted), and b=5.2 (dashed) which represent LCE1, LCE2, and LCE3 respectively.[29] (c) to (e) and (g) to (i) show the storage modulus G', the loss modulus G'', and dissipation tanδ = G''/G', of LCE1 and LCE3 respectively, determined through shear dynamic mechanical analysis at 1 rads^{-1}. (f) and (j) present an adhesion factor A = tanδ/G' determined from the shear DMA data. For c) to j), the different film alignments are identified through homeotropic (orange), planar ∥ (red), and planar ⊥ (green).

The different geometries in which it is possible to apply shear to SmA LCE films are shown in Figure 4 (a). The relationship between the smectic layer normal (and therefore the initial director) and the applied

shear has significant impact on the measured properties. In the homeotropic geometry, the layer normal is orthogonal to the shear, leading to an upper triangular deformation tensor (Equation (2))[13],

$$\underline{\underline{\lambda}} = \begin{pmatrix} \lambda_{xx} & 0 & \lambda_{xz} \\ 0 & \lambda_{yy} & 0 \\ 0 & 0 & \lambda_{zz} \end{pmatrix}. \quad \textbf{(2)}$$

Utilising volume conservation, $\lambda_{xx}\lambda_{yy}\lambda_{zz} = 1$, the free energy can be expressed as Equation (3):

$$F = \frac{1}{2}\mu\{\lambda_{xx}^2 + (\lambda_{xx}\lambda_{zz})^{-2} + \lambda_{zz}^2 + r\lambda_{xz}^2 + b(\lambda_{zz} - 1)^2\}. \quad \textbf{(3)}$$

There is no coupling between the applied shear and the smectic layer modulus, so the free energy minimises to (Equation (4)) where $\lambda_{xx} = \lambda_{zz} = 1$:

$$F = \frac{1}{2}\mu\{3 + r\lambda_{xz}^2\}. \quad \textbf{(4)}$$

This is the same as the nematic case, consequently there is no expected 'punishment' to the softness of the shear response in this geometry; it is expected to be analogous in nematic and SmA LCEs.

The planar ‖ geometry possesses the lower-triangular equivalent deformation tensor (Equation (5))[13]:

$$\underline{\underline{\lambda}} = \begin{pmatrix} \lambda_{xx} & 0 & 0 \\ 0 & \lambda_{yy} & 0 \\ \lambda_{zx} & 0 & \lambda_{zz} \end{pmatrix}. \quad \textbf{(5)}$$

The free energy now shows clear coupling between the applied shear and the evolution of the smectic layers (Equation (6)).

$$F = \frac{1}{2}\mu\left\{\lambda_{xx}^2 + \frac{1}{\lambda_{xx}^2\lambda_{zx}^2} + \lambda_{zx}^2 + \frac{\lambda_{zx}^2(\lambda_{xx}^2 + r\lambda_{zx}^2)}{\lambda_{xx}^2 + \lambda_{zx}^2} + b\left(\frac{\lambda_{xx}\lambda_{zx}}{\sqrt{\lambda_{xx}^2 + \lambda_{zx}^2}} - 1\right)^2\right\} \quad \textbf{(6)}$$

Minimising such an equation requires numerical methods and the solution when $r = 2.1$ and $b = 7.5$ is shown in Figure 4 (b). There is coupling between the shear and the layer spacing, which is manifest as an increased modulus[13]. To continue beyond a shear deformation of ~ 0.2 the deformation along the layer normal begins to increase, LCE1 requires a higher deformation than LCE2 and LCE3 – offering an explanation as to why LCE1 consistently fails whereas LCE2 and LCE3 do not. LCE2, with the lowest

layer spacing modulus, has a neglible increase in λ_{zz} and is able to accommodate large changes in strain which gives freedom for the auxetic response to occur.

Figure 4 (c-e, g-i) show the shear storage, G', and loss, G'', moduli measured for the SmA materials LCE1 and LCE3, together with the dissipation ratio, $tan\delta = G''/G'$, determined for an oscillation frequency of 1 rads^{-1} across the temperature range from 0 °C to 80 °C. The storage moduli take similar values for both materials plateauing above room temperature to values between around 0.1 – 1.0 MPa, but with a much higher anisotropy observed for LCE1 where the planar perpendicular case takes values around an order of magnitude higher than either of the other two geometries. The moduli are slightly higher than those reported for the nematic analogue of LCE1.[28] The loss factor, $\tan\delta$, shows a single peak that is associated with the glass transition at ~0 ˚C in both materials. An adhesion factor, correlated with the peel and tack strength of LCEs used as pressure sensitive adhesives, can be defined by Equation (7). The shear moduli are measured at small strain, and the assumption is made that the surface energy of each LCE type is the same across the geometries, which is valid for the nematic case.

$$A = \frac{\tan\delta}{G'(1\ rads^{-1})} = \frac{G''(1\ rads^{-1})}{(G'(1\ rads^{-1}))^2} \quad \textbf{(7)}$$

The adhesion factor is shown in Figure 4 (f) and (j), for LCE1 and LCE3 respectively. There is significant anisotropy in the adhesion factors, with the most dramatic variation observed between the homeotropic (stickiest) and planar perpendicular (least sticky) versions of LCE1 where there is a factor of ~20 difference between the two geometries. While the absolute values of the adhesion factor cannot be directly compared between the two materials because of the contributions of surface energy to adhesion, it is noteworthy that the homeotropic case for LCE1 is comparable in magnitude to the adhesion factor of the analogous nematic system.[28] This result is in keeping with both the chemical similarity of LCE1 and

the material considered by Street *et al.*[28] (the side group has a 6- rather than 8-carbon spacer) as well as the theoretical explanations presented earlier (Equation (4)), where the shear behaviour in the homeotropic SmA case is seen to be the same as in the nematic case. Simply speaking, this result can be thought of as a consequence of the fact that a change in layer spacing is not needed to shear the homeotropic smectic LCE, unlike the planar cases. A final point to note is that these particular LCEs do not satisfy the Dahlquist criterion (G'<0.11 MPa and $T_g \sim 0$ °C) and so would not be suitable for use as PSAs at room temperature[28,34], however the anisotropy in adhesion is starkly different to nematics which suggests that smectic adhesives may be an avenue for future PSA design.

Discussion and Conclusions

When considering the results presented herein as a whole, this work offers compelling considerations for both the controlled fabrication of smectic LCEs, as well as new approaches to the design of materials for applications. The prediction by de Gennes that templating smectic macromolecules in either nematic or smectic solvents stated for the two cases[†]:

1. *'if the chains are elongated in the direction of the nematic axis, we obtain, during crosslinking, a system stretched in this direction. But, during washing, the network can relax without major obstacle towards an isotropic conformation'; and*
2. *'in the smectic case where the chains are intercalated between the layers of the solvent, we would obtain ⋯ a very anisotropic material from the mechanical point of view.'*

We have tracked the evolution of the order present in the LCEs formed in a nematic solvent throughout the fabrication process, allowing us to elucidate the mechanism behind the frustration in these LCEs. Our x-ray scattering results show that the smectic ordering develops during curing and is retained with a comparable correlation length after the removal of unreactive nematic solvent. Thus, we can confirm that the formation of smectic layers in the LCEs is a direct result of the curing process (case 1 above) and that

[†] The translation may be imperfect and there is some paraphrasing for conciseness.

283 we might expect the mechanical properties of such a system to differ significantly from both nematic
284 LCEs and smectic systems fabricated in case 2. This finding has exciting implications for the wider LCE
285 research field, suggesting that new LCE systems could be obtained that previously have not been
286 observed. As has been reported here, this could in turn lead to novel behaviours for LCEs, expanding their
287 scope for applications.

288 Further to increasing our understanding of the evolution of frustration in LCEs, this work presents
289 a new family of LCEs with negative Poisson's ratio, explicitly showing that auxetic behaviour at a
290 molecular level is not limited to nematic LCEs[8,9,35]. Three of the smectic formulations reported are
291 sufficiently robust to allow strain into an auxetic regime. In all of these cases, the LCE was formed in a
292 non-smectic precursor mixture and we suggest that the frustrated nature of the resulting SmA LCE is in
293 part responsible for the ability to achieve high strains and therefore observe auxeticity. It has been
294 established that the threshold strain at which the auxetic response is observed in nematic LCEs is
295 dependent on dynamics, particularly the proximity to the glass transition temperature (T_g) of the
296 sample[8,33]. This manifests as materials with lower T_g exhibiting a lower auxetic threshold, when strained
297 at a given temperature[8]. The situation appears to be more complex in these auxetic SmA LCEs as
298 lowering T_g doesn't necessarily result in a lower auxetic threshold.

299 It is clear that one of the 'nematic-like' behaviours that can be retained in SmA LCEs is the
300 potential to deform biaxially and therefore exhibit auxeticity. We have also shown through the shear
301 moduli for two chemically similar LCEs (LCE1 and the material reported by Street *et al.*[28]), have
302 comparable moduli in the homeotropic case. Although the anisotropic adhesion factors were considerably
303 lower than have been observed in nematic LCEs, it is reasonable to suggest that approaches such as
304 increasing spacer lengths which will modify T_g might be exploited in order to produce pressure sensitive
305 SmA LCE adhesives that are able to satisfy the Dahlquist criterion. Indeed, the smectic nature of the
306 LCEs ensure a high anisotropy in the adhesion factors, potentially opening new avenues in LCE adhesive
307 development that utilise smectics.

Methods

Materials

The 8-(4-Cyano-biphenyl-4'-yloxy)octyl acrylate (M1) used in this work was synthesised in accordance with previous literature.[8] The 4-[[6-(Acryloyloxy)hexyl]oxy]benzoic acid (A6OBA) was purchased from Sigma Aldrich (Guangzhou, China), dissolved in dichloromethane (DCM), and filtered through a 0.22 μm syringe filter to remove insoluble impurities. All other materials were used as purchased without further purification, and were obtained from one of the following suppliers: Sigma Aldrich (Gillingham, UK), Fisher Scientific (Loughborough, UK), Apollo Scientific (Stockport, UK), Ambeed (Arlington Heights, IL, USA), Fluorochem (Glossop, UK), Synthon Chemicals GmBH (Wolfen, Germany).

LCE Mold Fabrication

The LCEs were synthesized in bespoke moulds, which were made in accordance with previous literature[5,8,10]. For the planar samples, glass microscope slide (7.5 cm x 2.5 cm x 1 mm), and a Melinex® ST725 substrate (7 cm x 2.5 cm x 250 μm) (DuPont Teijin Films, Redcar, UK) were spin coated on one surface with an aqueous 0.5 wt % polyvinyl alcohol (PVA) solution. After drying the coated substrates at 50 °C for 10 minutes, the substrates were uniaxially rubbed with a bespoke rubbing machine. These two substrates were then adhered, via Melinex® 401 spacers (7.5 cm x 0.2 cm x 100 μm) (DuPont Teijin Films, Redcar, UK) and UVS-91 adhesive, so that the PVA-rubbed surfaces were the inner surfaces of the constructed cell, and the rubbing directions yielded antiparallel planar alignment along the width of the mould. The adhesive was then cured by irradiation under 350 nm (2.5 Wcm-2) at 50 °C for 10 minutes, to yield the constructed LCE mould with a gap of ~100 μm thickness. For the homeotropic samples, the construction is identical except that the substrates also had ITO electrodes and a homeotropic alignment

agent, Cetyltrimethylammonium Bromide (CTAB) was used in place of the PVA.[10] A voltage applied during polymerisation (40 V_{rms}) supported the homeotropic alignment in the 100 μm thick layer.[10]

LCE Film Synthesis

LCE1, LCE2, and LCE3 were fabricated in accordance with previous literature[8,12], from the generalised mixtures displayed in Figure 2. In a typical procedure, 2-Methyl-1,4-phenylene bis(4-((6-(acryloyloxy)hexyloxy)benzoate (RM82) (3.5 mol%), the appropriate monofunctional monomer (M1/M2/M3)(24.4 mol%), and 4'-Hexyloxy-(1,1'-biphenyl)-4-carbonitrile (6OCB) (54.6 mol%) were heated to 120 °C with stirring until a homogeneous isotropic phase was obtained. The mixture was cooled to 45 °C, followed by the addition of 2-ethylhexyl acrylate (EHA) (16 mol%) and methylbenzoyl formate (MBF) (1.5 mol%), and stirred for 5 minutes, ensuring a homogeneous, completely isotropic material was obtained. The precursor mixtures for LCE1, LCE2, and LCE3 all exhibited only nematic phases with the transition to the isotropic phase, T_{NI}, reported in Table S1. The mixture was then filled into a mould at 50 °C via pipette, before being cooled to room temperature (23 ˚C) and allowed to stand for 30 minutes. The samples were then cured in the nematic phase under 350 nm (2.5 Wcm^2) irradiation for 2 hours. After curing, the samples were removed from the moulds (using a small amount of isopropanol if necessary to aid delamination from the substrates), and left to stand in a solution of DCM:isopropanol (30:70) overnight to remove the non-reactive 6OCB. The samples were then allowed to dry under ambient conditions for 5 hours, to yield the LCE films.

LCE4 was fabricated using the strain-induced alignment methodology frequently employed in the literature.[36,37] A mixture of RM82 (2.5 mol%), 6OBA (5 mol%), A6OCB (51 mol%), EHA (40.3 mol%) and MBF (1.2 mol%) was heated to 85°C and filled into the LCE mould. The sample was then cured at 85 ˚C under 350 nm (2.5 Wcm^2) irradiation for 2 hours. The polymerized sample was then heated to 100 °C and strained to 60% (1.6x times its original length) to induce liquid crystalline order and cooled to room temperature to lock the alignment.

Material Characterisation

X-Ray

Small- (SAXS) and Wide- (WAXS) angle X-ray scattering experiments were performed on an Anton Paar SAXSpoint 5.0 system (K-α Cu source, λ=1.5418 Å) with a Dectris EIGER2 R 1M (1028 pixel x 1062 pixel array) detector. For LCE films, measurements were performed at room temperature on ~100 μm thick samples averaging 3 frames with exposures times of 300 seconds. For the precursor mixture, the nematic fluid was held in a QGCT 1.0 quartz capillary (1.0 mm diameter) (Capillary Tube Supplies Ltd., Cornwall, UK), averaging 3 frames with exposure times of 300 seconds each. A 2 mm beam size was used. A background scan was performed for both the SAXS and WAXS detector position which was subtracted from the measurements to minimise contributions from intrinsic background scattering and the Mylar protective film in front of the detector.

The correlation lengths parallel ($\xi_{//}$) to the director were deduced from SAXS data, according to Equation (8), as was recently used by Kennedy *et al.* for LCEs[38]. This equation uses the full width half maximum ($w_{//}$) of Gaussian fittings to the scattering intensity of the q ~ 1.6 nm-1 feature (the (001) Bragg peak due to the smectic layer spacing).

$$\xi_{||} = \frac{2\pi}{w_{||}} \tag{8}$$

The scalar nematic order parameter, *S*, was calculated from the 2D WAXS pattern using the Kratky method[39] shown in Equation (9):

$$I(\chi) = f_0 + \frac{1}{2} f_2 \cos^2(\chi) + \frac{3}{8} f_4 \cos^4(\chi) + \frac{5}{16} f_6 \cos^6(\chi) + \frac{35}{128} f_8 \cos^8(\chi) + \frac{63}{256} f_{10} \cos^{10}(\chi) \dots , \tag{9}$$

Where I is intensity, χ is the azimuthal angle orthogonal with respect to the nematic director and f_n are constants determined by fitting equation (9). The f_n constants are used to determine $\langle \cos^2(\beta) \rangle$ through equation (10):

$$\langle \cos^2(\beta) \rangle = \frac{\sum_{n=0}^{\infty} \frac{f_{2n}}{2n+3}}{\sum_{n=0}^{\infty} \frac{f_{2n}}{2n+1}}, \quad (10)$$

where β is the angle between the axis of a molecule and the nematic director. Thus $S = \langle P_2 \rangle$ can be determined through the equation (11):

$$S = \frac{1}{2}(3\langle \cos^2(\beta) \rangle - 1)\,. \quad (11)$$

In calculating S, the baseline was removed using a zero-offset method.

Strain-strain behaviour and measurements of Poisson's ratio

A bespoke mechanical strain apparatus which has been described in detail in previous publications[5] consisting of two actuators capable of extending a sample with a minimum step size of 0.5 mm was used to determine the strain-strain behaviour of the LCE films. The apparatus allows for polarising microscopy and bright field images to be taken of the top-down view of the LCE, enabling a semi-quantitative analysis of the material optical properties incuding birefringence and transparency as a function of strain. LCE strips of approximate dimensions 20 mm x 2 mm x 100 μm were strained until failure at a rate of 0.05 mm min^{-1}. Features in the LCE were tracked using imageJ to deduce the strain in the length and the thickness of the film, and a constant volume condition used to determine the strain in the thickness. The instantaneous Poisson's ratio is deduced from the strain data as described in detail previously.[10]

Dynamic Mechanical Analysis

A TA Instruments Dynamic Mechanical Analysis 850, equipped with steel shear sandwich clamps, was used to shear two square samples of length 7 mm and thickness 100 μm using a centre movable plate. All

measurements were in the linear viscoelastic range, as confirmed by performing an initial strain sweep. A shear oscillatory frequency of 1 $rads^{-1}$ and temperature range of 80 °C cooling to 0 °C was used. All experiments were performed three times, with a representative dataset chosen for analysis.

Data Availability

Data is available for public access under the DOI: https://doi.org/10.5518/1726.

Acknowledgements

A.S thanks Pilkington Technology Management Ltd. And the University of Leeds. S.R.B, E.J.C, Z.W and H.F.G are grateful to the Engineering and Physical Sciences Research Council for funding through grant EP/V054724/1. All authors would also like to acknowledge the Engineering and Physical Sciences Research Council grant number EP/X0348011 for the purchase of the SAXS/WAXS system used in this work

Author Contribution Statement

"A.S, S.R.B, J.M, H.F.G" conceptualisation, "S.R.B, Z.W." sample preparation, "A.S, S.R.B, Z.W. J.M, H.F.G" methodology, "A.S, S.R.B" data curation, "A.S, S.R.B, E.J.C., H.F.G" draft preparation, "A.S, S.R.B, E.J.C., Z.W., J.M, H.F.G" review and editing, "J.M, H.F.G" supervision, "H.F.G" funding acquisition

Competing Interests

S.R.B., Z.W., H.F.G., have filed a patent related to auxetic smectic LCEs. All remaining authors declare no competing interests.

References

1. Evans, K. E. Auxetic polymers: a new range of materials. *Endeavour* **19**, 170–174 (1991).
2. Ren, X., Das, R., Tran, P., Ngo, T. D. & Xie, Y. M. Auxetic metamaterials and structures: A review. *Smart Mater. Struct.* **27**, 023001 (2018).

3. A. Turincio. Puma enters new era with cushioning technology Xetic. Puma SE,. *https://about.puma.com/en/newsroom/news/puma-enters-new-era-cushioning-technology-xetic* (2020).

4. Head GmbH. Auxetic 2.0 - The Science Behind the Sensational Feel. HEAD Sport GmbH,. https://www.head.com/en/rs/stories/auxetic-the-science-behind-the-sensational-feel (2026).

5. Mistry, D. *et al.* Coincident molecular auxeticity and negative order parameter in a liquid crystal elastomer. *Nat. Commun.* **9**, 5095 (2018).

6. Cooper, E. J. *et al.* Controlling the Optical Properties of Transparent Auxetic Liquid Crystal Elastomers. *Macromolecules* **57**, 2030–2038 (2024).

7. Moorhouse, T. & Raistrick, T. Sub-Micron Diffractive Optical Elements Facilitated by Intrinsic Deswelling of Auxetic Liquid Crystal Elastomers. *Adv. Opt. Mater.* **12**, 2400866 (2024).

8. Berrow, S. R., Raistrick, T., Mandle, R. J. & Gleeson, H. F. Structure–Property Relationships in Auxetic Liquid Crystal Elastomers—The Effect of Spacer Length. *Polymers (Basel).* **16**, 1957 (2024).

9. Berrow, S. R., Raistrick, T., Mandle, R. J. & Gleeson, H. F. Auxetic Liquid Crystal Elastomers: Overcoming Barriers to Scale-Up. *ACS Appl. Polym. Mater.* **7**, 4517–4524 (2025).

10. Wang, Z. *et al.* Direct Observation of Biaxial Nematic Order in Auxetic Liquid Crystal Elastomers. *Materials* **16**, 393 (2023).

11. Raistrick, T., Zhang, Z., Mistry, D., Mattsson, J. & Gleeson, H. F. Understanding the physics of the auxetic response in a liquid crystal elastomer. *Phys. Rev. Res.* **3**, 023191 (2021).

12. Berrow, S. R. *et al.* The effect of templating on the mechanical properties of smectic liquid crystal elastomers. *J. Mater. Chem. C Mater.* **13**, 12365–12375 (2025).

13. Adams, J. M. & Warner, M. Elasticity of smectic-A elastomers. *Phys. Rev. E Stat. Nonlin. Soft Matter Phys.* **71**, 021708 (2005).

14. Adams, J. M. & Warner, M. Soft elasticity in smectic elastomers. *Phys. Rev. E Stat. Nonlin. Soft Matter Phys.* **72**, (2005).

15. Warner, M. & Terentjev, E. M. *Liquid Crystal Elastomers*. (Oxford University PressOxford, Oxford, 2003).

16. De Gennes, P. G. Possibilities Offertes Par La Reticulation De Polymeres En Presence D'un Crystal Liquide. *Phys. Lett.* **28A**, 725–727 (1969).

17. Volume 7: Supermolecular and Polymeric Liquid Crystals. in *Handbook of Liquid Crystals* (eds. Goodby, J. W. et al.) vol. 4 (Wiley-VCH, Weinheim, 2014).

18. De Gennes, P. G. Reflexions sur un type de polymeres nematiques. *C R Acad Sci Ser, B* **281**, 101–103 (1975).

19. Clarke, S. M. *et al.* Soft elasticity and mechanical damping in liquid crystalline elastomers. *J. Appl. Phys.* **89**, 6530–6535 (2001).

20. Merkel, D. R., Shaha, R. K., Yakacki, C. M. & Frick, C. P. Mechanical energy dissipation in polydomain nematic liquid crystal elastomers in response to oscillating loading. *Polymer (Guildf).* **166**, 148–154 (2019).

21. Saed, M. O. *et al.* Impact damping and vibration attenuation in nematic liquid crystal elastomers. *Nat. Commun.* **12**, (2021).

22. Terentjev, E. M. Liquid Crystal Elastomers: 30 Years After. *Macromolecules* **58**, 2792–2806 (2025).

23. Lagerwall, J. Liquid crystal elastomer actuators and sensors: Glimpses of the past, the present and perhaps the future. *Programmable Materials* **1**, 1–46 (2023).

24. Guin, T. *et al.* Layered liquid crystal elastomer actuators. *Nat. Commun.* **9**, 2531 (2018).

25. Ohzono, T., Saed, M. O. & Terentjev, E. M. Enhanced Dynamic Adhesion in Nematic Liquid Crystal Elastomers. *Adv. Mater.* **31**, 1902642 (2019).

26. Pranda, P. A. *et al.* Directional Adhesion of Monodomain Liquid Crystalline Elastomers. *ACS Appl. Mater. Interfaces* **16**, 6394–6402 (2024).

27. Choi, S. *et al.* Harnessing Extreme Internal Damping in Polyrotaxane-Incorporated Liquid Crystal Elastomers for Pressure-Sensitive Adhesives. *Adv. Funct. Mater.* **35**, (2025).

28. Street, A., Mistry, D., Mattsson, J. & Gleeson, H. F. Geometry-Dependent Adhesion in Transparent Monodomain Liquid Crystal Elastomers. *Adv. Funct. Mater.* e22644 (2025).

29. Mistry, D. *et al.* Isotropic Liquid Crystal Elastomers as Exceptional Photoelastic Strain Sensors. *Macromolecules* **53**, 3709–3718 (2020).

30. Guo, H., Saed, M. O. & Terentjev, E. M. Mechanism of Pressure-Sensitive Adhesion in Nematic Elastomers. *Macromolecules* **56**, 6247–6255 (2023).

31. Leadbetter, A. J., Frost, J. C., Gaughan, J. P., Gray, G. W. & Mosley, A. The structure of smectic A phases of compounds with cyano end groups. *J. Phys. France* **40**, 375–380 (1979).

32. Berrow, S. R., Mandle, R. J., Raistrick, T., Reynolds, M. & Gleeson, H. F. Toward Monodomain Nematic Liquid Crystal Elastomers of Arbitrary Thickness through PET-RAFT Polymerization. *Macromolecules* **57**, 5218–5229 (2024).

33. Raistrick, T. *et al.* Resolving the mechanical response of liquid crystal elastomers – semi-soft elastic or auxetic. *Soft Matter* **21**, 8849–8866 (2025).

34. Chang, E. P. Viscoelastic Windows of Pressure-Sensitive Adhesives. *J. Adhes.* **34**, 189–200 (1991).

35. Liu, M. & Zhao, Y. Unusual Stretching-Induced Molecular Orientation Behavior of a Side-Chain Liquid Crystal Elastomer and Its Reorientation-Enabled Auxeticity. *Macromolecules* **58**, 905–918 (2025).

36. Herbert, K. M. *et al.* Synthesis and alignment of liquid crystalline elastomers. *Nat. Rev. Mater.* **7**, 23–38 (2022).

37. Ding, J. *et al.* Locking Alignment of Liquid Crystal Actuators Using Hydrogen Bonds to Enable Room-Temperature Shape Programmability and Enhanced Work Capacity. *Adv. Funct. Mater.* **35**, (2025).

38. Kennedy, D. T., Hoang, J. D., Toney, M. F. & White, T. J. Deconvoluting the Contribution of Polymerization Temperature to Liquid Crystalline Elastomer Actuation. *Macromolecules* **57**, 10032–10040 (2024).

39. Sims, M. T., Abbott, L. C., Richardson, R. M., Goodby, J. W. & Moore, J. N. Considerations in the determination of orientational order parameters from X-ray scattering experiments. *Liq. Cryst.* **46**, 11–24 (2019).

Tables

Table 1. The correlation length, smectic layer spacing and order parameters of the LCEs for each formulation, elucidated from X-ray scattering measurements. In the case of LCE1, the evolution of these parameters throughout the fabrication process (i.e. unwashed film vs final LCE) is given.Values in brackets () show the error in the reported values of order parameter.

Material	**Correlation length (Å / Nº of layers)**	**SmA layer spacing (Å)**	**Order parameter**
LCE1 unwashed film	205 / 6	34	0.62 (±0.03)
LCE1	161 / 5	41	0.56 (±0.03)
LCE2	100 / 2	45	0.61 (±0.03)
LCE3	119 / 3	41	0.61 (±0.03)
LCE4	189 / 4	48	0.59 (±0.03)

Supplementary Files

This is a list of supplementary files associated with this preprint. Click to download.

- SIFrustratedSmectics.docx